

SAND97-2460C

Submitted for inclusion in 21st Aging, Compatibility and Stockpile Stewardship Conference

CONF-970982--

SAND-97-2460C

Evaluation of the Metal/Adhesive Interfaces in the MC2370 Fire Set

RECEIVED

Kevin R. Zavadil

Sandia National Laboratories

Albuquerque, New Mexico 87185

OCT 15 1997

OSTI

Abstract

Several analysis methods have been applied to evaluate the structure and composition of the electrode/adhesive interfaces in previously fielded M2370 Fire Sets. A method of interfacial fracture at cryogenic temperatures as been employed to expose regions of these interfaces at multiple levels in a SFE stack. Electron microscopy shows that bond failure induced by the fracture is predominantly adhesive with an equal probability of failure at the Au and Cu interfaces. Some evidence for cohesive failure exists in transition regions where the fracture has moved between interfaces. Pinhole structure is evident in a majority of the adhesive, indicative of a possible microstructure related to electrical breakdown. Pinhole-free larger regions of adhesive also exist which may explain the observed high resistance in impedance measurements.

Introduction

Slim loop ferroelectric (SFE) fire sets are constructed in a laminate form with a copper foil electrode adhered to a lead barium zirconate titanate (PBZT) ceramic dielectric (1). A 20 μm layer of a room temperature cured silicone adhesive (RTV511) is used to establish intimate contact between the foil electrode and a thin sputter deposited gold film (with a Cr adhesion layer) on the PBZT. The adhesive must be made sufficiently electrically conductive to support both rapid charge accumulation and release at the Au/PBZT interface. In addition, conductivity must be maintained over the expected lifetime of the fire set to ensure effective operation. Concerns exist for the stability of the silicone and its electrode interfaces (both Au and Cu). Silicones are known to undergo slow reversion and cyclization reactions due to the presence of the active Sn(IV) catalyst used in the curing process. In addition, residual volatile species like methanol (produced during polymerization) and mobile oxidants like water present opportunities for chemical oxidation of the metal electrode surfaces with time. These processes could eventually lead to degradation in the electrical contact to the SFE and a resulting change in performance of the fire set.

Our goal has been to investigate the likelihood of chemical and structural changes in the interfacial regions of the SFE structure. A combination of methods have been applied to extract this information from MC2370 units recovered from dismantled W68 systems at the Pantex facility. Transmission ultrasonic images of these units shows a variable degree of acoustic transmission between units as well as spatially within a given unit (2). The absence of regions of total transmission loss indicates that large scale interfacial disbonding does not occur in these units. The potential contribution of losses at the external interfaces of the structure, those that do not contribute to the electrical performance of the unit, have been eliminated as a cause of low transmission using a pulse echo technique. Frequency dependent capacitance and dissipation factor data shows that some units with low acoustic transmission yield lower than expected capacitance values and higher than expected dissipation factor values (2). In a simple RC circuit analog, these result translate to a high series resistance leading to SFE capacitor. In light of these results, attempts have been made to gain an understanding of the structure and composition of the interfaces and how these change with component aging.

Results and Discussion

Low temperature fracture has been used to extract the adhesive/ electrode interface. Figure 1 shows the resulting fragments of a fracture at approximately -150°C (liquid N₂ immersion) using a knife edge that was manually forced parallel to the center layer of an SFE stack. A cryogenic process has been employed to ensure brittle failure in the adhesive below its glass transition temperature (-115°C). The bright planar features in the photograph are opposing

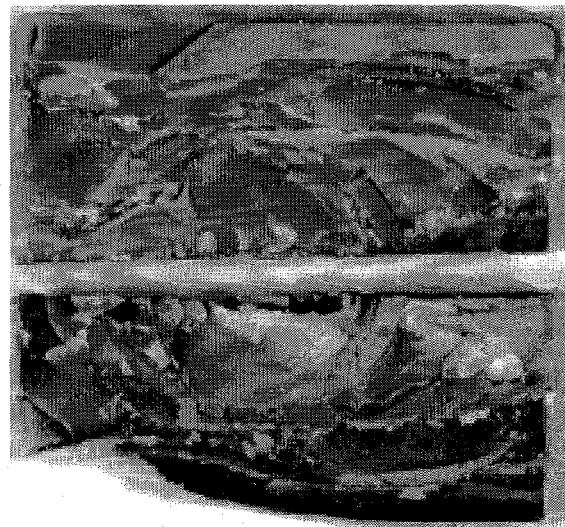


Figure 1: Cold Fractured SFE Stack

DISTRIBUTION OF THIS DOCUMENT IS UNLIMITED

MASTER

DISCLAIMER

Portions of this document may be illegible in electronic image products. Images are produced from the best available original document.

DISCLAIMER

This report was prepared as an account of work sponsored by an agency of the United States Government. Neither the United States Government nor any agency thereof, nor any of their employees, make any warranty, express or implied, or assumes any legal liability or responsibility for the accuracy, completeness, or usefulness of any information, apparatus, product, or process disclosed, or represents that its use would not infringe privately owned rights. Reference herein to any specific commercial product, process, or service by trade name, trademark, manufacturer, or otherwise does not necessarily constitute or imply its endorsement, recommendation, or favoring by the United States Government or any agency thereof. The views and opinions of authors expressed herein do not necessarily state or reflect those of the United States Government or any agency thereof.

Cu and Au electrode surfaces. The conical fracture features are a result of mechanical failure of the PBZT which shows an extreme extent of fracture propagation lateral to the direction of force. Despite the fact that fracture was not confined to a single layer, we can use microspectroscopic imaging and analysis techniques to learn about the way electrodes were bonded and to search for evidence of microstructure.

Secondary electron imaging coupled with energy dispersive x-ray analysis provides specific information on interface structure. Figure 2a and 2b shows a set of micrographs acquired from opposing fractured faces (see Fig. 1). The fracture process has exposed an electrode region several millimeters in width and extending several centimeters in length. These secondary images show bright emission from the electrode region in Fig. 2a and attenuated emission in Fig. 2b. X-ray analysis demonstrates that the bright image in 2a is the Au electrode while the darker region in 2b is adhesive covered Cu, based on Si K shell emission. The adherence of the silicone to Cu during the fracture indicates adhesive failure at the interface. The darker regions that show up on the Au electrode can be matched with brighter emission regions on the Cu electrode, specifically at both the cusp that appears in the upper right hand corner and along the upper step of Figure. 2a. These features are produced by silicone adhesion to the Au and indicate that the fracture process can propagate across the adhesive moving from side-to-side of the electrode/adhesive/electrode structure. The particulate structure that shows up on the Au and silicone surfaces is predominantly PBZT debris that is produced by the fracture process.



Figure 2a and 2b: Secondary Electron Micrographs Showing Opposing Fracture Faces - left image (a) is the Au electrode, right image (b) is the silicone covered Cu electrode

The predominant fracture mechanism appears to be adhesive. No clear trend exists showing a greater tendency for failure at the Au versus the Cu interface. However, regions of the electrode interface do exist where evidence of cohesive failure is apparent. Figure 3 shows a backscattered electron micrograph of a transition region along a Au surface. The mesa structure at the top of the image is the edge of the silicone while the highly textured region at the micrograph base is the sputter deposited Au electrode. This image was generated by selective biasing of the four quadrant detector to highlight topography. The center region of the micrograph shows considerable residual silicone filling in the large areas of the nodular Au microstructure. The plane of fracture has clearly moved out into the adhesive layer in this transition region and has become significantly more cohesive. Similar observations have been made on select areas for the Cu electrode. However, the Cu electrode possesses much less intrinsic texture preventing a microstructural determination of cohesive failure. Large scale variation in the relative intensities for Si K and Cu L shell emission measured on adhesive covered Cu regions indicate varying adhesive layer

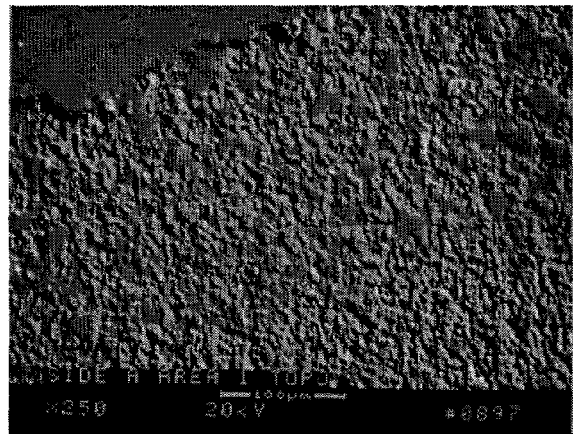


Figure 3: Backscattered Electron Micrograph of a Transition Region Showing Cohesive Failure

thickness. These findings suggest that local cohesive failure can occur in this system.

Additional types of structure show up in the adhesive that might be indicative of electrical property variation. Figure 4 show a secondary electron image of a typical region of adhesive exposed by the fracture method. The adhesive is perforated with a moderate density of pinholes that vary in diameter from approximately 1 to 20 μm . These pinholes are assumed to be a result of electrical breakdown of the adhesive when the units are exposed to short 450 to 500 V pulses. This value of voltage corresponds to an exposure of 50% the field strength of the adhesive (20.5 kV/mm) and, given the 20 μm layer thickness, could result in catastrophic local breakdown of the silicone. Electrical conduction might be supported by carbonization of the adhesive adjacent to the pinhole. These pinholes are not observed in all regions of the adhesive. If these pinhole signify ohmic paths, their absence in large enough regions could require that more charge flow must be supported by the several thousand angstrom thick Au electrode over longer lateral distances, resulting in the larger series resistance indicated by impedance measurements.

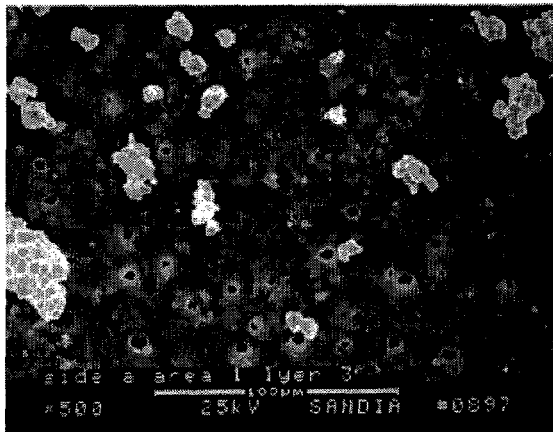


Figure 4: Micrograph Showing Pinholes in the RTV511 Adhesive

Methods of more controlled interfacial fracture are currently being developed for these systems in order to extract larger regions of the interface. The goal will be to correlate the low acoustic transmission and high series resistance with the existence of these pinholes and with surface analytical information derived from x-ray photoelectron spectroscopy and secondary ion mass spectrometry. In addition, experiments are underway to use a microprobe technique to evaluate and map the extent of carbonization radially outward from a pinhole to verify their role in electrical breakdown.

Conclusions

SFE laminate stacks from MC2370 fire sets have been subjected to cryogenic, interfacial fracture. Secondary and backscattered electron images show that bond failure is predominately adhesive with no specific preference for failure at either the Au or Cu electrode. Evidence for occasional cohesive failure exists in transition regions where the plane of fracture shifts between adjacent electrodes. Energy dispersive x-ray analysis has been used to confirm the presence or absence of silicone adhesive at the electrode surface. Pinholes are observed in a majority of the exposed adhesive that range in both size and distribution. Pore diameters as small as 1 μm and as large as several tens of μm have been observed. These pinholes are most likely the result of electrical breakdown of the adhesive under test conditions of 50% the field strength of RTV511. Regions of adhesive have been observed where these pores are essentially non-existent. Large scale variation in ohmic paths through the adhesive may explain the large series resistance determined from capacitance measurements.

Acknowledgments

This work was performed at Sandia National Laboratories and supported by the U.S. Department of Energy under Contract No. DE-AC04-94-AL85000.

References:

1. J.O. Harris and R.L. Maxwell, "MC2370 SFE Firing Set Development Report," SC-DR-70-353, 1971
2. W.L. Warren, B.A. Tuttle and D. Dimos, "Aging of the Slim Loop Ferroelectric Material in the MC3028 and MC2370 Fire Sets," Final Report to R. Salzbrenner, 1997.